Aminoalkyl-Substituted Indenylnickel(II) Complexes (η^3:η^0-Ind$(CH_2)_2NMe_2$)Ni$(PR_3)X$ and [(η^3:η^1-Ind$(CH_2)_2NMe_2$)Ni(PR_3)][BPh_4]: Influence of the Phosphine in Ligand Exchange and Polymerization Reactions

Laurent F. Groux and Davit Zargarian*

Département de Chimie, Université de Montréal, Montréal (Québec), Canada H3C 3J7

Received August 26, 2003

Reaction of LiInd$(CH_2)_2NMe_2$ with $(PR_3)_2NiCl_2$ gave the neutral complexes (η^3:η^0-Ind$(CH_2)_2$-NMe_2)Ni(PR_3)Cl (R = Ph (**1**) or Me (**2**)), while the PCy_3 analogue, (η^3:η^0-Ind$(CH_2)_2NMe_2$)-Ni(PCy_3)Cl (**3**), was obtained by reacting **1** with PCy_3. These Ni−Cl species react with R′Li or $NaBPh_4$ to form, respectively, the corresponding Ni−R′ derivatives (η^3:η^0-Ind$(CH_2)_2NMe_2$)-Ni(PR_3)R′ (R = Ph, R′ = Me (**4**) or CCPh (**5**); R = R′ = Me (**6**)) or the cationic species [(η^3:η^1-Ind$(CH_2)_2NMe_2$)Ni(PR_3)]$^+$ (R = Ph (**7**), Me (**8**), or Cy (**9**)), in which the NMe_2 moiety is coordinated to the nickel center. These complexes have been fully characterized, including solid state structure determinations by X-ray crystallography for complexes **2**, **4**, **5**, **6**, and **9**. Inspection of the structural data showed that replacing the Cl ligand by the more strongly donating ligands CCPh and Me reinforces the Ni−P and Ni−Ind interactions. On the other hand, electrochemical measurements showed that the reduction potentials of the Ni−Cl compounds are intermediate between the Ni−R′ derivatives, which are more resistant to reduction, and the cationic species, which are the easiest to reduce. The cationic complexes are single-component catalysts for the polymerization of styrene, giving poly(styrene) with M_w in the range of 10^4−10^5, and the hydrosilylation of styrene and 1-hexene with $PhSiH_3$ and Ph_2SiH_2. The nature of the phosphine ligand has an important influence on the catalytic reactivities, the PMe_3 analogue **8** being the most active catalyst.

Introduction

An important class of hemilabile ligands consists of functionalized cyclopentadienyl ligands represented by Cp^L, with ^ denoting the side chain linking the Cp ligand to a functional group L such as NRR′,[1] OR,[2] PRR′,[3] SR,[3] AsRR′,[3] and C=C.[4] The main role of the Cp moiety is to anchor these multidentate ligands to metal centers, while the reversible coordination of L modulates the reactivities of the metal center. In principle, substrates can displace the hemilabile group L from the metal center in order to initiate reactivity; on the other hand, since L is never far from the metal, it can re-coordinate readily in the absence of substrate to prevent the decomposition of the catalyst (Scheme 1). The potential of this class of compounds in catalysis has spurred research efforts in this area and resulted in the preparation of many transition metal complexes bearing Cp^L type ligands or their indenyl analogues. Examination of the reactivities of some of these complexes has demonstrated the dramatic influence of the hemilabile ligands in improving catalytic reactivities, stabilizing otherwise unstable species, changing solubility properties, introducing chirality, and so on.[5]

Scheme 1

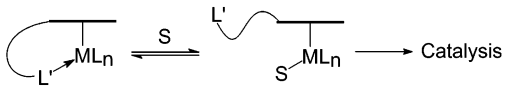

We became interested in this area of research during our investigations on the catalytic reactivities of indenyl−nickel(II) complexes.[6] What inspired us to examine the influence of a hemilabile moiety in our complexes was the observation that the highly reactive, in situ generated cationic species [IndNi$(PR_3)]^+$ (Ind = indenyl and its substituted derivatives) are rapidly converted to the inactive compounds [IndNi$(PR_3)_2]^+$ in the absence of substrates. The presence of this deactivation pathway meant that these catalysts had to be generated in situ and in the presence of a large excess of substrate; otherwise, the formation of the bis(phosphine) derivatives would inhibit the catalysis. We reasoned that the incorporation of a hemilabile moiety in the vicinity of the Ni center might circumvent catalyst deactivation, thereby improving catalyst lifetimes.

(1) Review on Cp^NRR′ ligands: Jutzi, P. *Eur. J. Inorg. Chem.* **1998**, 663.
(2) Review on Cp^OR ligands: Siemeling, U. *Chem. Rev.* **2000**, *100*, 1495.
(3) Review on Cp^L (L = PRR′, AsRR′, and SR) ligands: Butenschoen, H. *Chem. Rev.* **2000**, *100*, 1527.
(4) General review on functionalized Cp ligands: Müller, C.; Vos, D.; Jutzi, P. *J. Organomet. Chem.* **2000**, *600*, 127.
(5) For reviews of this topic see: (a) Müller, C.; Vos, D.; Jutzi, P. *J. Organomet. Chem.* **2000**, *600*, 127. (b) Jutzi, P.; Redeker, T. *Eur. J. Inorg. Chem.* **1998**, 663. (c) Jutzi, P.; Siemeling, U. *J. Organomet. Chem.* **1995**, *500*, 175. (d) Jutzi, P.; Dahlaus, J. *Coord. Chem. Rev.* **1994**, *137*, 179.
(6) Zargarian, D. *Coord. Chem. Rev.* **2002**, *233*−*234*, 157.

10.1021/om0341348 CCC: $25.00
Publication on Web 10/09/2003

This assertion was borne out by the results of studies on the influence of an amino tether on the reactivity of the complexes.[7] Thus, we found that the cationic complexes $[(\eta^3{:}\eta^1\text{-Ind}\text{^}NR_2)Ni(PPh_3)]^+$ were active, single-component catalysts (i.e., no activation or in situ generation needed) for polymerization of styrene and norbornene. Interestingly, the M_w and solubilities of the products obtained from these reactions were different from those of the products obtained from reactions promoted by the in situ generated $[(Ind)Ni(PPh_3)]^+$, implying that the hemilabile moiety might also influence the course of the catalysis.[7b] Isolation and complete characterization of the new complexes, as well as a study of their ligand exchange reactions, allowed an evaluation of the N→Ni binding as a function of the incoming ligand's nucleophilicity[7a] and different amine substituents.[7d]

As a follow up to our previous studies, we have prepared analogous cationic compounds with PMe_3 and PCy_3 instead of PPh_3 in order to examine the influence of the phosphine ligand on the binding of the tether to the Ni center and on the reactivities of these complexes. The present report describes the preparation and characterization of the chloro derivatives $(\eta^3{:}\eta^0\text{-Ind}(CH_2)_2NMe_2)Ni(PR_3)Cl$ (R = Me (**2**) and Cy (**3**)), the cationic complexes $[(\eta^3{:}\eta^1\text{-Ind}(CH_2)_2NMe_2)Ni(PR_3)]^+$ (R = Me (**8**) and Cy (**9**)), and $(\eta^3{:}\eta^0\text{-Ind}(CH_2)_2NMe_2)Ni(PR_3)R'$ (R = Ph, R′ = Me (**4**) and CCPh (**5**); R = R′ = Me (**6**)). The catalytic reactivities of these compounds in the polymerization of styrene and phenylacatylene, oligomerization of $PhSiH_3$, and the hydrosilylation of styrene and 1-hexene are also reported herein.

Results and Discussion

Synthesis and Spectroscopic Characterization. The previously reported[7a] preparation of $(\eta^3{:}\eta^0\text{-Ind}(CH_2)_2NMe_2)(PPh_3)Ni-Cl$, **1**, served as a model for the synthesis of $(\eta^3{:}\eta^0\text{-Ind}(CH_2)_2NMe_2)(PMe_3)Ni-Cl$, **2**. Thus, slow addition of 1 equiv of $LiInd(CH_2)_2NMe_2$ to 1 equiv of $Ni(PMe_3)_2Cl_2$ in THF gave a dark red solution, from which pure **2** precipitated gradually. On the other hand, the PCy_3 analogue $(\eta^3{:}\eta^0\text{-Ind}(CH_2)_2NMe_2)(PCy_3)Ni-Cl$, **3**, was readily obtained by adding 1.5 equiv of PCy_3 to a solution of **1** in Et_2O (Scheme 2).

The new complexes have been fully characterized by NMR spectroscopy (^1H, ^{13}C, and ^{31}P), elemental analysis, and in the case of **2** X-ray diffraction studies. The NMR spectra of complexes **2** and **3** display the characteristic signals observed for the analogous nonfunctionalized compounds $(1\text{-Me-Ind})Ni(PR_3)Cl$ (R = Ph, Me, Cy).[8] For instance, the $^{31}P\{^1H\}$ NMR spectra showed singlets for the phosphine ligands at −11 ppm for **2** (cf. −10.6 ppm for its 1-Me-Ind analogue) and 37.0 ppm for **3** (cf. to 37.2 ppm for its 1-Me-Ind analogue). The ^1H and $^{13}C\{^1H\}$ NMR spectra also served to establish the degree of N→Ni interaction in these complexes, as described below.

Scheme 2 [a]

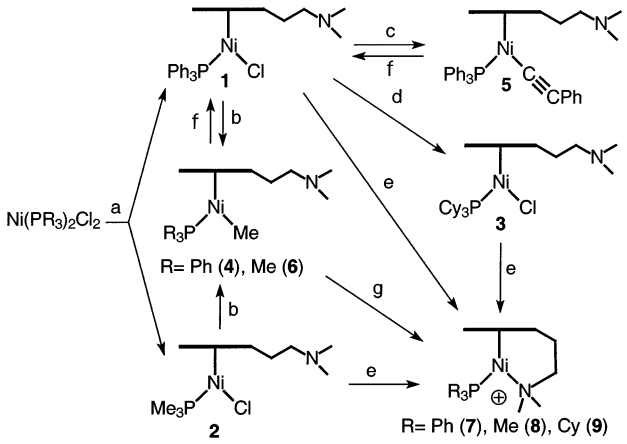

[a] a = $LiInd(CH_2)_2NMe_2$; b = LiMe; c = LiCCPh; d = PCy_3; e = $NaBPh_4$; f = HCl; g = HBF_4.

Previous studies had shown that the complexes $(Ind\text{^}NR_2)PPh_3Ni(Cl)$ display variable degrees of dynamic N→Ni binding: temperature-dependent ^1H and $^{13}C\{^1H\}$ NMR spectra were obtained, with the room-temperature ^1H NMR spectra displaying very broad signals, while the corresponding $^{13}C\{^1H\}$ NMR spectra contained few of the expected resonances. In the case of complexes **2** and **3**, however, no signal broadening was observed in the ^1H NMR spectra and all the anticipated ^{13}C NMR resonances were accounted for. Moreover, the $N(CH_3)_2$ groups in these complexes were found to be equivalent, which indicates that the amine moiety was not coordinating to the Ni center. (Since these complexes have C_1 symmetry, N→Ni coordination would be expected to render the Me groups chemically inequivalent.) Therefore, we conclude that complexes **2** and **3** do not undergo a dynamic exchange process involving amine chelation, in contrast to their previously studied PPh_3 analogues. This difference is presumably related to the higher electron density of the Ni center in **2** and **3**, which is in turn brought about by the more strongly donating phosphines PMe_3 and PCy_3. This issue will be addressed in the next section, along with the solid state structure of **2**.

The chloro complexes **1**−**3** have been used to prepare the new Ni−Me and Ni−CC−Ph derivatives $(\eta^3{:}\eta^0\text{-Ind}(CH_2)_2NMe_2)Ni(PR_3)R'$ (R = Ph, R′ = Me (**4**) and CCPh (**5**); R = R′ = Me (**6**)) and the chelated cations $[(\eta^3{:}\eta^1\text{-Ind}(CH_2)_2NMe_2)Ni(PR_3)]^+$ (R = Me (**8**) and Cy (**9**)). The main motivation for preparing the neutral, nonchelating derivatives was an earlier observation that seemed to indicate that even when the amine moiety in the precatalysts is not chelated, its proximity to the Ni center seems to have a marked influence over the course of the catalytic reactions and the nature of their products. Thus, the Ni−Me derivatives **4** and **6** were obtained by reacting MeLi with **1** or **2**, respectively, while the Ni−CCPh derivative **5** was prepared in a similar manner by the metathetic reaction between **1** and LiCCPh (Scheme 2); recrystallization of the crude products from hexane gave pure compounds. Reacting these compounds with HCl gives back the Ni−Cl precursors.

The new complexes were characterized by NMR spectroscopy, and their solid state structures were determined by X-ray crystallography.[9] For instance, the

(7) (a) Groux, L. F.; Bélanger-Gariépy, F.; Zargarian, D.; Vollmerhaus, R. *Organometallics* **2000**, *19*, 1507. (b) Groux, L. F.; Zargarian, D. *Organometallics* **2001**, *20*, 3811. (c) Groux, L. F.; Zargarian, D.; Simon, L. C.; Soares, J. B. P. *J. Mol. Catal. A: Chem.* **2003**, *193*, 51. (d) Groux, L. F.; Zargarian, D. *Organometallics* **2003**, *22*, 3124.

(8) (a) Huber, T. A.; Bayrakdarian, M.; Dion, S.; Dubuc, I.; Bélanger-Gariépy, F.; Zargarian, D. *Organometallics* **1997**, *16*, 5811. (b) Fontaine, F.-G.; Dubois, M.-A.; Zargarian, D. *Organometallics* **2001**, *20*, 5156.

Scheme 3

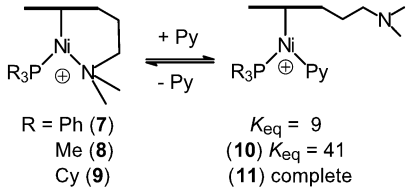

$^{31}P\{^1H\}$ NMR spectra showed singlets for the phosphine ligands at 46.9 ppm for **4** (cf. 47.7 ppm for its 1-Me-Ind analogue),[8a] 38.8 ppm for **5** (cf. 40.4 for its 1-Me-Ind analogue),[10] and −4.0 ppm for **6** (cf. −3.7 ppm for its 1-Me-Ind analogue).[11] In addition, the characteristic doublet resonances for the Ni−CH_3 moieties in **4** and **6** were observed at −0.65 ppm (**4**, $^3J_{P-H}$ = 5.6 Hz) and −0.73 ppm (**6**, $^3J_{P-H}$ = 6.3 Hz) in the ^1H NMR spectra and −18.3 ppm (**4**, $^2J_{P-C}$ = 24.8 Hz) and −21.7 ppm (**6**, $^2J_{P-C}$ = 25.2 Hz) in the $^{13}C\{^1H\}$ NMR spectra. As before, the equivalence of the N(CH_3)$_2$ groups confirmed the absence of any Ni−N interactions. On the other hand, the absorption signal for ν(CC) in the IR spectrum of **5** appeared at 2099 cm^{-1}, very close to the corresponding signals in the 1-Me-Ind analogue (2090 cm^{-1})[10] and free phenylacetylene (2110 cm^{-1}), implying little or no Ni−CCPh back-bonding in these complexes. The results of the X-ray diffraction studies will be discussed in the next section.

The cationic complexes **8** and **9** were prepared in analogy with their PPh_3 analogue, **7**,[7b] by reacting the chloro precursors with $NaBPh_4$ or the Ni−Me precursor **6** with HBF_4 (Scheme 2); these new complexes were purified by multiple recrystallizations from Et_2O/CH_2Cl_2 mixtures. The $^{31}P\{^1H\}$ NMR spectra of these compounds displayed one new singlet resonance at ca. −20.8 ppm for **8** and ca. 24.9 ppm for **9**; the absence of AA′ doublet resonances in these spectra indicated that formation of the corresponding bis-phosphine complexes had been circumvented by the chelation of the amine moiety. On the other hand, the N→Ni chelation was supported by the observed inequivalence of IndCH_2CH_2N(CH_3)$_2$ signals and confirmed by the solid structure of **9**, which is discussed below.

Solid State Structures and Electrochemical Studies. Suitable crystals for X-ray diffraction studies were obtained for **2**, **4**, **5**, **6**, and **9**, as described in the Experimental Section, and studied at 223 K. The details of data collection and the structure refinement parameters are listed in Table 1, while bond distances and angles are reported in Table 2. The overall geometry in all of the complexes studied can be described as distorted square planar, with the Ind moiety occupying two coordination sites and the largest distortion arising from the small C1−Ni−C3 angle of ca. 67°.[6] In complexes **2**, **4**, **5**, and **6**, no Ni−N interaction is detected: the NMe_2 moiety is pointed away from the Ni, extending along the plane of coordination (as in **2**, **4**, and **6**) or almost perpendicular to it (as in **5**). The different orientation of the amine moiety is likely a result of packing interactions, and we have seen that complex **1** can adopt one or the other structure depending on crystallization conditions.[12]

The Ni−Ind interaction is fairly symmetrical (Ni−C1 ≈ Ni−C3; Ni−C3a ≈ Ni−C7a) in the Ni−Me complexes **4** and **6**, quite unsymmetrical in **2** (Ni−C1 > Ni−C3), and somewhat unsymmetrical in **5** (Ni−C1 > Ni−C3 by greater than 13 esd) and **9** (Ni−C1 < Ni−C3 by about 15 esd). As described in detail elsewhere,[6] these observations can be attributed to the relative trans influences of the PR_3 and X ligands in the neutral complexes (X = Cl, Me, CCPh, etc.) or the geometrical constraints imposed by the chelation in the cationic species. The Ind hapticity, as measured by the slip parameter Δ(M−C),[13] seems to vary as a function of PR_3 basicity, showing a higher Ind hapticity (i.e., smaller Δ(M−C)) in **1** (0.23 Å)[7a] versus **2** (0.32 Å), **4** (0.18 Å) versus **6** (0.20 Å), and **7** (0.26 Å) versus **9** (0.32 Å). On the other hand, for complexes having the same phosphine ligand, the Ind hapticity increases (i.e., Δ(M−C) decreases) with the stronger basicity of the X ligand, as follows: **1** < **5** < **4**; **2** < **6**.

The Ni−alkynyl bond length in **5** (1.852(4) Å) is much shorter than the Ni−Me distances in **4** (1.9508(17) Å) and **6** (1.983(4) Å), presumably because of the greater sp character of the alkynyl carbon. On the other hand, the Ni−P distances are shortest in the Ni−Me complexes (ca. 2.13 Å) compared to the Ni−Cl and Ni−CCPh complexes (ca. 2.16 Å) or the cationic complex **9** (ca. 2.24 Å). This observation prompted us to compare the Ni−PPh_3 bond lengths as a function of the ligand X in the complexes Ind$Ni(PPh_3)X$, many of which have been characterized structurally.[6] This comparison confirmed a trend in the Ni−P bond distances, which are shorter in the Ni−alkyl derivatives (ca. 2.12−2.13 Å), followed by derivatives of other anionic ligands such as chloro, alkynyl, phthalimidato, and thienyl (ca. 2.16−2.19 Å),[6] and the cations featuring the chelating amino moieties (ca. 2.20 in **7**[7b] and ca. 2.22 Å in [{η^3:η^1-IndCH_2(2-pyridine)}Ni(PPh_3)]$^+$).[7d] A similar trend is noted for the Ni−Ind interactions, which are stronger (i.e., the slip parameter Δ(M−C) is smaller) with the Ni−Me derivative **4**, followed by the Ni−Cl derivative **1** and the cationic **7**.

In the search for a relationship between the above-noted structural trends and the relative electron richness of these complexes, we undertook electrochemical studies, with the following results. Cyclic voltammetry measurements of complexes **1**−**9** showed that they undergo irreversible reductions at potentials ranging from −1.16 to −2.33 V (vs SCE), as reported in Table 3. Inspection of the electrochemical data shows the following:

(a) As expected, the cationic species are more easily reduced than the neutral complexes.

(b) The E_{red} values for the cationic species **8** (−1.22 V) and **7** (−1.16 V) follow the donor ability of the phosphine (PMe_3 > PPh_3), but the reduction potential

(9) It should be noted, however, that the results of combustion analysis for complex **6** were not acceptable, leading us to suspect that this compound is thermally unstable with respect to the reductive coupling of the Ind^NMe_2 and the methyl ligands.

(10) Wang, R.; Bélanger-Gariépy, F.; Zargarian, D. *Organometallics* **1999**, *18*, 5548.

(11) Fontaine, F.-G.; Zargarian, D. *Organometallics* **2002**, *21*, 401.

(12) Groux, L. F.; Zargarian, D. *Acta Crystallogr.* **2001**, *E57*, m547.

(13) The slip parameter, Δ(M−C), is determined according to the relationship (M−C3a + M−C7a)/2 − (M−C1 + M−C3)/2. Thus, a Δ-(M−C) value of 0 would signal a perfectly η^5 coordination of Ind, whereas increasing degrees of slippage toward η^3 coordination would result in larger values: (a) Baker, R. T.; Tulip, T. H. *Organometallics* **1986**, *5*, 839. (b) Westcott, S. A.; Kakkar, A.; Stringer, G.; Taylor, N. J.; Marder, T. B. *J. Organomet. Chem.* **1990**, *394*, 777.

Table 1. Crystal Data, Data Collection, and Structure Refinement Parameters

	2	**4**	**5**	**6**	**9**
formula	$C_{16}H_{25}NPNiCl$	$C_{32}H_{34}NPNi\cdot Hex$	$C_{39}H_{36}NPNi\cdot THF$	$C_{17}H_{28}NPNi$	$C_{55}H_{69}NBPNi\cdot CH_2Cl_2$
cryst color	dark red	dark red	dark red	dark red	dark red
cryst habit	needle	block	block	needle	block
cryst dimens, mm	0.78 × 0.13 × 0.07	0.96 × 0.40 × 0.26	0.46 × 0.24 × 0.13	0.84 × 0.08 × 0.08	0.17 × 0.20 × 0.20
symmetry	monoclinic	triclinic	triclinic	triclinic	triclinic
space group	$P2_1/n$	$P\bar{1}$	$P\bar{1}$	$P\bar{1}$	$P\bar{1}$
a, Å	6.3037(2)	9.3419(3)	9.998(3)	6.4485(2)	10.9625(1)
b, Å	15.6826(5)	12.8669(5)	13.887(4)	8.5720(3)	13.4241(2)
c, Å	18.2702(6)	13.9322(5)	14.716(5)	16.7049(5)	17.6136(2)
α, deg	90	98.748(3)	111.58(3)	84.18(3)	83.939(1)
β, deg	96.106(2)	103.145(2)	99.68(3)	80.64(3)	87.023(1)
γ, deg	90	106.493(3)	99.55(3)	85.70(3)	78.308(1)
volume, Å^3	1795.92(10)	1521.01(10)	1814.2(10)	904.77(5)	2522.84(5)
Z	4	2	2	2	2
D(calcd), g cm^{-1}	1.3185	1.2345	1.2349	1.234	1.224
diffractometer	Bruker AXS SMART 2K	Bruker AXS SMART 2K	Nonius CAD-4	Bruker AXS SMART 2K	Bruker AXS SMART 2K
temp, K	223(2)	223(2)	223(2)	223(2)	223(2)
λ (Cu Kα), Å	1.54178	1.54178	1.54178	1.54178	1.54178
μ, mm^{-1}	3.677	1.576	1.489	2.290	2.094
scan type	*ω* scan	*ω* scan	*ω*/2*θ* scan	*ω* scan	*ω* scan
θ_{max} (deg)	72.75	72.64	69.93	72.62	72.95
h,*k*,*l* range	$-6 \le h \le 7$ $-19 \le k \le 19$ $-22 \le l \le 22$	$-11 \le h \le 11$ $-15 \le k \le 14$ $-17 \le l \le 17$	$-12 \le h \le 12$ $-16 \le k \le 16$ $-17 \le l \le 17$	$-7 \le h \le 7$ $-10 \le k \le 10$ $-20 \le l \le 20$	$-13 \le h \le 13$ $-16 \le k \le 16$ $-21 \le l \le 21$
reflns used ($I > 2\sigma(I)$)	2927	5440	4139	3405	7639
abs correction	multiscan SADABS	multiscan SADABS	integration ABSORB	multiscan SADABS	multiscan SADABS
T (min, max)	0.398, 0.773	0.389, 0.662	0.5977, 0.8501	0.464, 0.833	0.620, 0.700
$R[F^2>2\sigma(F^2)]$, $wR(F^2)$	0.0363, 0.0967	0.0411, 0.1153	0.0428, 0.0948	0.0751, 0.1961	0.0441, 0.1268
GOF	1.003	1.086	1.014	1.005	1.011

Table 2. Selected Bond Distances (Å) and Angles (deg) for 2, 4, 5, 6, and 9

	2	**4**	**5**	**6**	**9**
Ni−P	2.1608(6)	2.1277(5)	2.1573(11)	2.1290(12)	2.2424(5)
Ni−X[a]	2.1868(6)	1.9508(17)	1.852(4)	1.983(4)	2.022(5)
Ni−C1	2.1184(19)	2.0870(17)	2.092(2)	2.100(3)	2.0660(18)
Ni−C2	2.0389(19)	2.0810(17)	2.061(3)	2.090(4)	2.0466(19)
Ni−C3	2.0344(19)	2.1012(16)	2.051(3)	2.081(4)	2.096(2)
Ni−C3A	2.3817(19)	2.2659(15)	2.283(3)	2.285(3)	2.4172(19)
Ni−C7A	2.4035(18)	2.2811(16)	2.280(3)	2.294(3)	2.3932(19)
C1−C2	1.406(3)	1.421(2)	1.413(3)	1.418(5)	1.419(3)
C2−C3	1.419(3)	1.409(2)	1.395(4)	1.420(6)	1.408(3)
C3−C3A	1.468(3)	1.441(2)	1.454(4)	1.445(6)	1.463(3)
C3A−C7A	1.417(3)	1.429(2)	1.428(4)	1.430(5)	1.413(3)
C7A−C1	1.467(2)	1.456(2)	1.445(4)	1.467(5)	1.461(3)
C1−C8	1.495(3)	1.503(2)	1.493(3)	1.516(5)	1.503(5)
Δ(M−C)[b]	0.32	0.18	0.21	0.20	0.32
C1−Ni−X[a]	97.78(5)	94.39(7)	94.02(14)	96.90(15)	82.70(17)
P−Ni−X[a]	95.86(2)	93.23(6)	95.64(12)	93.18(11)	111.11(16)
P−Ni−C3	99.48(6)	107.25(5)	103.60(8)	103.05(12)	100.45(6)
C1−Ni−C3	66.92(8)	66.68(6)	66.88(11)	66.66(15)	66.42(8)
C3−Ni−X[a]	163.78(6)	157.91(8)	160.71(14)	162.69(16)	148.08(18)
P−Ni−C1	166.36(5)	168.83(5)	169.81(8)	169.59(11)	165.24(6)
N−C9−C8	113.42(15)	113.53(14)	115.4(3)	113.0(3)	109.8(4)
C1−C8−C9	110.75(16)	110.89(14)	116.5(2)	111.8(3)	107.4(4)
HA[c]	12.5(2)	8.2(2)	9.6(3)	9.4(2)	12.6(2)
FA[d]	13.2(2)	7.5(2)	9.2(3)	7.3(2)	13.2(2)

[a] X = Cl, C12, or N. [b] Δ(M−C) = {Ni−C_{av} (for C7a and C3a) − Ni−C_{av} (for C1 and C3}. [c] HA = angle between C1/C2/C3 plane and C1/C3/C3A/C7A plane. [d] FA = angle between C1/C2/C3 plane and C3A/C4/C5/C6/C7/C7A plane.

of the PCy_3 analogue **9** is only slightly more negative (−1.17 V) than that of the PPh_3 analogue; this might be due to the greater steric volume of PCy_3 that results in a very long Ni−P bond and, presumably, a less effective electron donation.

(c) The Ni−Me derivatives have more negative reduction potentials than their Ni−Cl counterparts: −2.33 V (**4**) versus −1.41 V (**1**); −2.12 V (**6**) versus −1.27 V (**2**). The E_{red} value for the Ni−CCPh derivative **5** (−1.72 V) is intermediate between those of its chloro and cationic analogues.

Therefore, the electrochemical measurements are in fairly good agreement with the solid state data and signal a correlation between the apparent electron-richness of the Ni center and its interactions with the phosphine and Ind ligands.[14] On a first approximation, the above observations indicate that the most electron-rich Ni centers (i.e., those with the strongly donating alkyl ligands) form the shortest Ni−P bonds and the strongest Ni−Ind interactions, whereas the longest Ni−P bonds and weakest Ni−Ind interactions occur with the least electron rich centers (i.e., the cationic

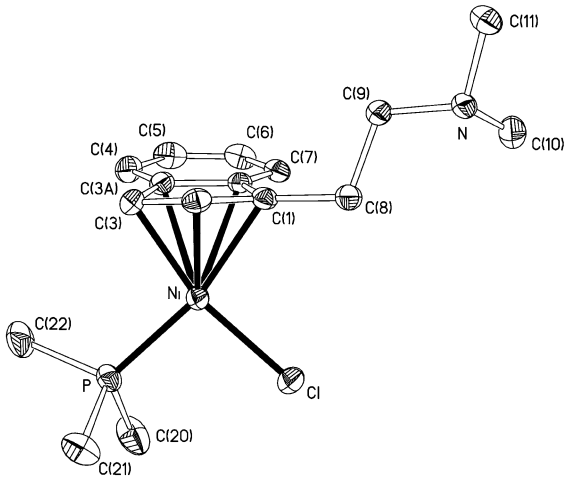

Figure 1. ORTEP plot of **2**. Hydrogen atoms are omitted for clarity.

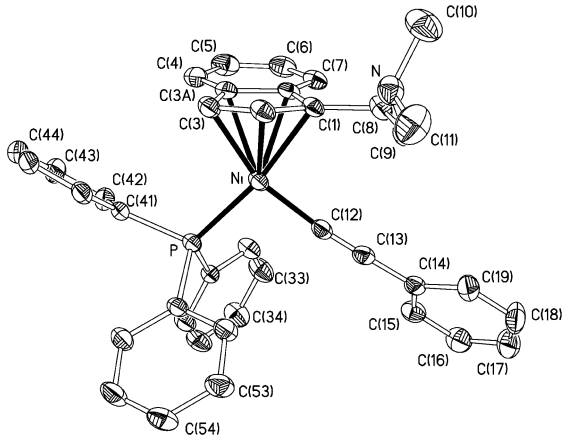

Figure 2. ORTEP plot of **4**. Hydrogen (except on the Ni-Me) and solvent atoms are omitted for clarity.

Table 3. Characterization of Complexes 1−9

	$^{31}P\{^1H\}$ (ppm)	^1H (ppm)				E_{Red} (V vs SCE)
		H2	H3	H4	E_{Red}[a] (V obs)	
1[b]	30.8	6.70	3.42	6.11	−1.70	−1.41
2[b]	−11.0	6.57	3.66	6.59	−1.56	−1.27
3[b]	37.0	6.76	4.17		−1.96	−1.67
4[b]	46.9	6.39	4.22	6.54	−2.62	−2.33
5[c]	38.8	6.45	3.97	6.14	−2.01	−1.72
6[b]	−4.0	6.24	4.47	6.99	−2.41	−2.12
7[c]	29.1	6.78	3.94	5.54	−1.45	−1.16
8[d]	−20.8	6.79	4.29	6.78	−1.51	−1.22
9[d]	24.9	7.15	4.41	6.79	−1.46	−1.17

[a] CH_3CN. [b] C_6D_6. [c] $CDCl_3$. [d] CD_2Cl_2.

species). This correlation is evident from a graph of Δ(M−C) values and Ni−P distances against the E_{red} values (Figure 6). We have also noted an empirical correlation between the two structural parameters (Ni−P distances and Δ(M−C) values) and the reduction potentials of these complexes, on one hand, and their ^{31}P chemical shifts, on the other (Table 3). Thus, the Ni−Me derivatives and the cations show the most downfield and upfield shifts, respectively, whereas the Ni−Cl and Ni−CCPh deriviatves have intermediate shifts, as follows (δ values given in ppm): for PMe_3 complexes, **6** (−4.0) > **2** (−11.0) > **8** (−20.8); for PCy_3

(14) Strictly speaking, the reduction potential of an irreversible reduction (or oxidation) process might vary as a function of many different parameters such as electrolyte composition and nature of electrode. It is common practice, however, to consider that in situations where an analogous series of compounds are being studied under identical conditions the values of reduction potential can be related, to a good approximation, to structural or electronic properties of the compounds. In the present case, since we are dealing with a family of complexes possessing very similar structural features and compositions, and since the electrochemical studies were performed under identical conditions, we believe that the reduction potential values represent fairly accurately the electron richness of the metal centers in this family of complexes.

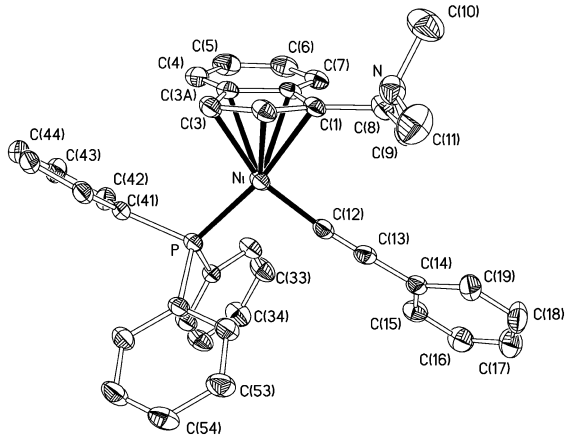

Figure 3. ORTEP plot of **5**. Hydrogen and solvent atoms are omitted for clarity.

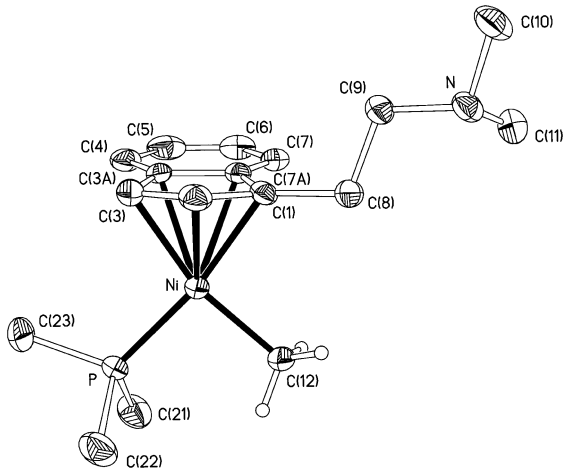

Figure 4. ORTEP plot of **6**. Hydrogen atoms are omitted for clarity except on the Ni-Me.

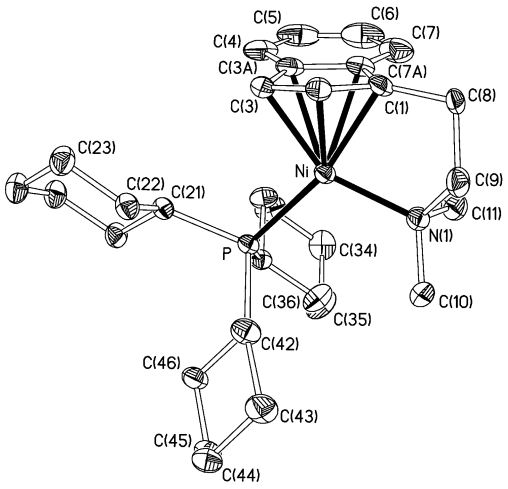

Figure 5. ORTEP plot of **9** with the major orientation of the tether. Hydrogen atoms, counterion, other orientation of the tether, and disordered CH_2Cl_2 are omitted for clarity.

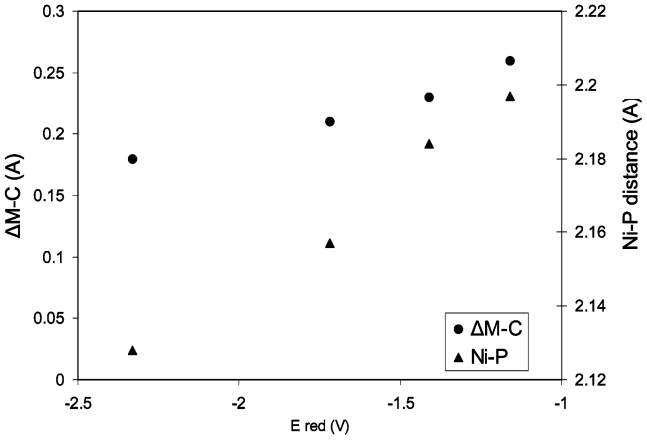

Figure 6. Correlation between electrodensity on the Ni and ligand donation.

complexes, **3** (37.0) > **9** (24.9); for PPh_3 complexes, **4** (46.9) > **5** (38.8) > **1** (30.8) > **7** (29.1).

The above findings may be explained in terms of the hard−soft acid−base theory (or the E−C model), as proposed by Bergman and co-workers[15] for the analogous Cp* complexes: when bonded to a soft ligand such as an alkyl group, the Ni center becomes softer and binds more effectively with other soft ligands such as PR_3 and Ind; conversely, when bonded to a hard ligand such as Cl in the neutral compounds or an amine in the cationic species, the Ni center binds less effectively with soft ligands, resulting in weaker Ni−P and Ni−Ind interactions. Whereas this explanation applies fairly well to all of the complexes studied here, alternative explanations involving Ni→P π-back-bonding and Cl→Ni π-donation account for the observed structural data in case of the PPh_3 and the chloro complexes only.[16]

Ligand Exchange Reactions. The hemilabile chelation of the tethered amine in the cationic complexes $[(\eta^3{:}\eta^1\text{-Ind}\text{^}NR_2)Ni(PR_3)]^+$ is particularly important in view of using these compounds as precatalysts. In this sense, the ease with which the N−Ni binding can be displaced by incoming substrates should have a direct bearing on the catalytic activities of these complexes. In our previous studies,[7b,d] we have measured the degree of Ni−N lability in some of these compounds using ligand exchange reactions. These studies showed that a number of strong ligands (e.g., pyridine, dppe, etc.) can displace the chelating amine moiety; this displacement is generally governed by an equilibrium process of which the K_{eq} depends on the relative nucleophilicities of the incoming ligand and the tethered amine. In addition, the activities of the cations in the polymerization of styrene were found to correlate with the lability of the N→Ni bond, more labile cases showing higher catalytic activities. (One exception was the complex bearing a pyridine moiety wherein Ni→N π back-bonding gave a stronger N→Ni interaction while displaying higher catalytic activity.) In the present study, we have performed similar studies in order to evaluate the influence of different phosphines on the lability of the Ni−N bonds and the relative effectiveness of these complexes in catalysis.

Initial tests showed that even relatively weak ligands such as styrene and norbornene displace the chelating NMe_2 moiety in **8** and **9**. To compare the Ni−N bonding strength in these and the previously studied complexes, we reacted **8** and **9** with increasing portions of pyridine (py) and monitored the ensuing equilibria by NMR spectroscopy. The new species $[(\eta^3{:}\eta^0\text{-Ind}(CH_2)_2NMe_2)Ni(PMe_3)(py)]^+$, **10**, formed in the equilibrium between py and complex **8**; the K_{eq} was determined to be 41 ± 6 M^{-1}, which is larger than the K_{eq} of 9 ± 1 M^{-1} found for the reaction of **7** with py. In the cases of complex **9**, only 1 equiv of py was sufficient for completely converting this complex into $[(\eta^3{:}\eta^0\text{-Ind}(CH_2)_2NMe_2)Ni(PCy_3)(Py)]^+$ (**11**). On the basis of these observations, the Ni−N binding strength in the cationic compounds follows the order **7** (PPh_3) > **8** (PMe_3) > **9** (PCy_3). Therefore, both the greater steric bulk of PCy_3 and the greater basicity of PMe_3 increase the lability of the Ni−N bond. As will be discussed in the next section, the relative catalytic activities of these complexes are largely reflected in the observed order of Ni−N bond lability.

Table 4. Polymerization Experiments

	cat.	monomer equiv	equiv	T (°C)	time (days)	M_w (10^{-3})	PDI	TON[c]
1	**7**[a]	styrene	2000	20	7			0
2	**7**[a]	styrene	2000	80	2	77.3	3.2	364
3	**8**	styrene	2000	20	2	38.1	2.9	23
4	**8**	styrene	2000	80	2	243.4	4.0	630
5	**9**	styrene	2000	20	2	11.6	1.8	57
6	**9**	styrene	2000	80	2	147.9	4.2	350
7	**7**, **8**, or **9**	PhCCH	100	20	1	no reaction		
8	**7**/MAO[b]	PhCCH	100	20	1	34.5	3.2	<10
9	**8**/MAO[b]	PhCCH	100	20	1	57.7	1.8	<10
10	**9**/MAO[b]	PhCCH	100	20	1	41.5	1.8	<10
11	**5**/MAO[b]	PhCCH	100	20	1	3.4	1.5	<10

[a] See ref 7b. [b] [Al]/[Ni] = 10. [c] Based on isolated yield.

Catalytic Polymerization Reactions. Previous studies[7b] had indicated that complex **7** is unreactive toward styrene at room temperature, but heating to 80 °C initiated the polymerization reaction; this requirement for heating was attributed to the difficulty of displacing the chelating NMe_2 moiety by styrene. Since **8** and **9** feature more labile Ni−N bonds, we set out to determine if the polymerization of styrene by these precatalysts would take place more readily. Indeed, complexes **8** and **9** do polymerize styrene at room temperature, but high levels of catalytic activity and large molecular weights are obtained only at higher temperatures (Table 4, runs 3−6). The level of catalytic activity in these reactions seems to be affected mainly by steric effects, the PMe_3 derivative **8** giving the

(15) Holland, P. L.; Smith, M. E.; Andersen, R. A.; Bergmann, R. G. *J. Am. Chem. Soc.* **1997**, *119*, 12815.

(16) One of the reviewers of our manuscript has suggested an alternative explanation for the structural observations, as follows. First, it is suggested that larger slip-fold distortions (i.e., larger ΔM−C values) of the Ind ligand should not be taken as an indication of weaker Ni−Ind bonds, because average Ni−C (Ind) bonds are shorter (and hence the Ni−Ind interaction is stronger) in the Ni−Cl derivatives (e.g., **2**) vs the Ni−Me derivatives (e.g., **6**). We disagree on the last point: the average Ni−C distance is smaller in **2** (2.064 vs 2.090 Å) only if we take into account the allyl portion of the Ind ligand; if, however, distances over all five Ind carbons are considered, the Ni−Me derivative **6** has shorter Ni−C bond lengths (2.170 vs 2.195 Å in **2**). In other words, the Ni−Ind interaction appears to be stronger in the system possessing the better donor (Me vs Cl). This reviewer also suggests that shorter Ni−P distances (and, by extension, stronger Ni−P bonds) be attributed to more extensive Ni→P π-back-bonding present in the more electron-rich complexes such as the Ni−Me derivative **6**. Although we do not rule out this possibility, it seems to us that PMe_3 is not well-known for significant π-back-bonding interactions with metals. Furthermore, it is not clear why this type of interaction would not take place in the Ni−Cl derivative wherein the Ind ligand could serve as a good source of electron density.

highest activity, while the PCy_3 derivative **9** and its PPh_3 analogue **7** displayed comparable activities. On the other hand, the M_w of the polymer appears to correlate with electronic effects: the precatalyst **8**, featuring the best donor phosphine ligand (and the compound with the most negative E_{red} value), gives polymers with the longest chains, followed by **9** and **7**. That longer polymer chain length and/or higher catalytic activity arise from systems having the better donating phosphines PCy_3 or PMe_3 suggests that the phosphine ligand remains coordinated to the Ni center during the polymerization reaction.

We have also examined the reactivities of complexes **7**, **8**, and **9** with phenylacetylene for the following reason. Previous studies[10,17] have shown that combining the precursors (1-Me-indenyl)Ni(PR_3)X (R = Ph or Cy, X = Cl, Me, CCPh, thienyl) with methylaluminoxane (MAO) forms catalytically active species that polymerize phenylacetylene to *cis,transoidal*-poly(phenylacetylene) (PPA); this material is of interest for applications requiring nonlinear optical and magnetic susceptibilities, photoconductivity, and gas permeability.[18] Although the interaction of MAO with these precursors gives rise to cationic species, the role of the latter in the polymerization reaction has not been established with certainty. In an earlier attempt to address this issue, we studied the reaction of phenylacetylene with (1-*i*-Pr-indenyl)(PPh_3)Ni(OTf) (OTf = OSO_2CF_3), a compound that can generate the unsaturated cations by the in situ displacement of the triflate anion.[19] This reaction gave poor yields of a polymeric material possessing lower solubility and diminished M_w compared to the samples obtained from the MAO-cocatalyzed reactions; these results implied that the cationic species present in the latter reactions are not be responsible for the formation of PPA. Access to the cationic complexes **7**, **8**, and **9** provided a good opportunity to further probe this question, as described below.

As shown in Table 4, the cationic complexes do not promote the polymerization of phenylacetylene (run 7). Given the earlier discussed lability of the Ni−N bond in complexes **8** and **9**, it is reasonable to presume that excess phenylacetylene should compete effectively with the chelating NMe_2 moiety for coordination to the Ni center; therefore, what hinders the polymerization in the absence of MAO is not the monomer's access to the Ni center. A more likely reason is that unlike the polymerization of styrene, which can proceed by an electrophilic pathway, the polymerization of phenylacetylene proceeds by an insertion mechanism requiring a Ni−R moiety for initiation; thus, the cationic Ni center must be converted into a neutral derivative possessing a moiety that can facilitate the initiation step. To test whether MAO could activate the cationic complexes, we carried out the polymerization of phenylacetylene in the presence of MAO (ca. 1:10 ratio of Ni:Al); these reactions gave PPA having properties similar to those of the samples obtained from previous MAO-cocatalyzed reactions (Table 4, runs 8−10). The M_w of the polymers obtained from these reactions are comparable to the values obtained with previously studied systems not bearing tethered amine moieties on the Ind ligand, but the activities of the present systems are inferior.

In an attempt to gain insight on how MAO activates the cationic complexes, we monitored the NMR spectra of a mixture consisting of **7** (ca. 0.015 M in CD_2Cl_2) and 10 equiv each of MAO and phenylacetylene. The $^{31}P\{^1H\}$ NMR spectrum showed the conversion of **7** to the analogous Ni−Me and Ni−CCPh derivatives, as evidenced by the singlet resonances at 45.5 and 39.9 ppm, respectively; evidently, MAO can bring about the formation of the requisite Ni−R moieties. We were intrigued to find, however, that polymerization reactions using combinations of MAO and independently prepared (as opposed to in situ formed) samples of the Ni-Me and Ni−CCPh derivatives **4** and **5**, respectively, yielded PPA samples with much lower M_w values (e.g., see run 11 for the reaction of **5** + MAO). Since the combination of MAO and the analogous neutral Ni−R derivatives (R = Me or CCPh) bearing nonfunctionalized Ind ligands polymerize phenylacetylene,[10,18] it is clear that the amine moiety has a detrimental effect on these reactions. We conclude, therefore, that the cationic species cannot polymerize phenylacetylene in the absence of MAO, but the precise role of the latter in these reactions remains unknown.

Olefin Hydrosilylation Reactions. The complexes Ind(PR_3)Ni(X), either used directly (X = alkyl) or generated in situ (X = H or positive charge), are known to catalyze the dehydrogenative oligomerization of $PhSiH_3$[11,20] and the hydrosilylation of olefins and ketones.[21] We have studied the influence of the tethered amine moiety on the course of these reactions, beginning with the reactivity of complexes **4**−**6** in the oligomerization of $PhSiH_3$. Thus, addition of neat $PhSiH_3$ (200 equiv) to solid samples of **4**−**6** caused an immediate evolution of gas (presumably H_2); ^1H NMR spectra of aliquots taken at various intervals showed the gradual conversion of the monomer to cyclic and linear $(PhSiH)_n$.[22] The viscous oil produced after 3 days was analyzed by NMR and GPC and found to consist primarily of cyclic and linear oligomers in ca. 3:1 ratio for **5** and 1:3 ratio for **4** and **6**. Qualitatively, the oligomers obtained from reactions promoted by complexes **4**−**6** and their nonfunctionalized counterparts are quite similar,[11] but the present precatalysts give higher conversions (monomer conversion was >95% in all cases).

Next, we examined the effectiveness of complexes **7**−**9** in the hydrosilylation of styrene and 1-hexene; most of the experiments were carried out at room temperature and on a NMR scale in CD_2Cl_2 using 100 equiv each of olefin and silane (Table 5). Analysis of the reaction

(17) Wang, R.; Groux, L. F.; Zargarian, D. *J. Organomet. Chem*, **2002**, *660*, 98.

(18) (a) Chien, J. C. W. *Polyacetylene Chemistry, Physics and Material Science*; Academic Press: New York, 1984. (b) Bredas, J. L.; Street, G. B. *Acc. Chem. Res.* **1985**, *18*, 309. (c) Masuda, T.; Higashimura, T. *Adv. Polym. Sci.* **1986**, *81*, 121. (d) Yoshimura, T.; Masuda, T.; Higashimura, T.; Ishihara, T. *J. Polym. Sci., Polym. Chem. Ed.* **1986**, *24*, 3569.

(19) Wang, R.; Groux, L. F.; Zargarian, D. *Organometallics* **2002**, *21*, 5531.

(20) Fontaine, F.-G.; Kadkhodazadeh, T.; Zargarian, D. *J. Chem. Soc., Chem. Commun.* **1998**, 1253−1254.

(21) (a) Fontaine, F.-G. Ph.D. Thesis, Université de Montréal, 2002. (b) Fontaine, F.-G.; Nguyen, R.-V.; Zargarian, D. *Can. J. Chem.* **2003**, in press.

(22) For details on the analysis of these materials by NMR see ref 11.

Table 5. Hydrosilylation of Olefins[a]

	cat.	olefin (equiv)	silane (equiv)	product (conversion, %)
1	**7**	styrene (100)	$PhSiH_3$ (100)	$Ph(PhSiH_2)CHCH_3$ (70)
2	**8**	styrene (100)	$PhSiH_3$ (100)	$Ph(PhSiH_2)CHCH_3$ (100)
3	**9**	styrene (100)	$PhSiH_3$ (100)	$Ph(PhSiH_2)CHCH_3$ (45)
4	**8**	styrene (1000)	$PhSiH_3$ (1000)	$Ph(PhSiH_2)CHCH_3$ (93)
5	**8**	styrene (100)	Ph_2SiH_2 (100)	$Ph(Ph_2SiH)CHCH_3$ (70) $PhCH_2CH_2SiHPh_2$ (10)
6	**8**	1-hexene (100)	$PhSiH_3$ (100)	1-$(PhSiH_2)$hexane (20)

products[23] obtained from the hydrosilylation of styrene with $PhSiH_3$ confirmed the exclusive formation of $Ph(PhSiH_2)CHCH_3$ with a conversion of 45% (**9**), 70% (**7**), and 100% (**8**) (Table 5, runs 1−3); no evidence was found for the formation of poly(styrene) or $(PhSiH)_n$. The reaction of complex **8** was repeated on a larger scale and found to give a very good catalytic turnover number (run 4). Replacing $PhSiH_3$ by Ph_2SiH_2 gave the α-addition isomer $Ph(Ph_2SiH)CHCH_3$ as the major product (70%) plus a small quantity (<10%) of the *β*-addition isomer $Ph(CH_2)_2SiHPh_2$ (run 5). Finally, reaction of 1-hexene with $PhSiH_3$ in the presence of **7** led to the formation of 1-$(PhSiH_2)$hexane with only 20% conversion (run 6).

The above results demonstrate that the cationic complexes **7**−**9** can act as single-component precatalysts for the hydrosilylation reaction. It is noteworthy that the presence of hydrosilanes in the reaction mixture inhibits the polymerization of styrene, while the presence of styrene inhibits or minimizes the dehydrogenative oligomerization of $PhSiH_3$. That the most active precatalyst is the one bearing the most strongly donating phosphine ligand (PMe_3) suggests that the hydrosilylation reaction does not involve phosphine dissociation; by inference, we believe that the catalysis involves the dissociation of the chelating amine moiety. Although the mechanistic details of this reaction are not known with certainty, a number of observations from previous studies[21] have pointed to the following sequence of steps: (a) the transfer of a hydride from the hydrosilane to the cationic Ni center forms a Ni−H intermediate; (b) insertion of the olefin gives a Ni−alkyl species; (c) a concerted, *σ*-bond metathesis reaction between the hydrosilane and the alkyl intermediate releases the hydrosilylation product and regenerates the Ni−H species. Precedent for the last step has been observed in our studies on the oligomerization of silanes.[11] In an attempt to extract mechanistic clues for the first two steps, we monitored near-stoichiometric reactions by NMR, with the following results.

No reaction took place between complex **8** (ca. 0.02 M in CD_2Cl_2) and styrene (5 equiv) over 2.5 h at room temperature, but addition of $PhSiH_3$ (5 equiv) to this sample resulted in the partial conversion of **8** to a new species displaying a $^{31}P\{^1H\}$ NMR signal at 32.7 ppm. Over time, two additional $^{31}P\{^1H\}$ NMR signals appeared (−5.8 and −8.3 ppm), but the starting material (−19.6 ppm) was still the major P-containing species even after 24 h. The ^1H NMR spectrum contained the characteristic signals of the reaction product $Ph(PhSiH_2)CHCH_3$, but the putative Ni−H species was not detected. In a similar experiment, $PhSiH_3$ was added to **8** first and the sample was studied by $^{31}P\{^1H\}$ NMR; in this case, three other signals emerged over a few hours (43.9, −2.8, and −8.1 ppm) in addition to the one at 32.7 ppm that had been observed in the previous experiment. Addition of styrene to this sample caused the immediate disappearance of the signals at 43.9, −2.8, and −8.1 ppm and gave rise to the same signals as in the previous experiment (32.7, −5.8, and −8.3 ppm) along with the signal for **8**. The ^1H NMR spectrum showed the formation of $Ph(PhSiH_2)CHCH_3$ as soon as the styrene was added.

The above results confirm that the first step in the hydrosilylation reaction takes place between the precursor and $PhSiH_3$ and generates at least four P-containing intermediate species. We believe that one of these intermediates is a Ni−H species formed via the transfer of H^- from $PhSiH_3$;[24] unfortunately, however, we were unable to detect the Ni−*H* signal in the ^1H NMR spectrum. This might be due to the weak intensity of this signal as a result of coupling to the P nucleus. To gain some indirect support for the conversion of complex **8** to a Ni−H species, we repeated the hydrosilylation reactions in $CDCl_3$; given the propensity of many metal hydrides to react with chloroform, we reasoned that the course of the hydrosilylation reaction should be affected in this medium. Indeed, these reaction mixtures turned dark blue immediately and the $^{31}P\{^1H\}$ NMR spectrum revealed two new signals at 40.7 and 38.9 ppm, but no trace of the hydrosilylation product was detected in the ^1H NMR spectrum. This observation is consistent with the postulated formation of Ni−H, but it does not validate it.

The postualted Ni−H intermediate would presumably promote the formation of Si−Si bonds in the absence of styrene, but insertion of styrene should form a Ni−alkyl species and drive the reaction toward hydrosilylation. This Ni−alkyl intermediate should exhibit a $^{31}P\{^1H\}$ NMR signal close to the corresponding signal for the Ni−Me complex **6** (−4.0 ppm); thus, of the $^{31}P\{^1H\}$ NMR signals detected at the end of the hydrosilylation reactions, those appearing at ca. −6 and −8 ppm might be due to the Ni−alkyl species.

Conclusion

The results of the present study on the chemistry of the complexes $[(\eta^3{:}\eta^1\text{-IndCH}_2\text{CH}_2\text{NMe}_2)\text{Ni}(\text{PR}_3)]^+$ demonstrate the influence of phosphine ligands on the hemilabile nature of the Ni−N bond and the reactivities of these complexes. Although the lability of the N→Ni binding, as measured by how easily the chelating amine moiety is displaced by pyridine, increases in the order $PPh_3 < PMe_3 < PCy_3$, the enhanced lability is not translated into superior catalytic activities in all cases. For instance, we found that the significant steric bulk of the PCy_3 ligand attenuates the impact of the hemilabile Ni−N moiety; as a result, the more labile Ni−N bond in the PCy_3 derivative does not confer a significant reactivity advantage to this complex relative to the PPh_3 derivative. On the other hand, the increased lability of the Ni−N bond is reflected in the superior catalytic activities of the complex bearing the strongly donating and relatively nonbulky phosphine PMe_3. The results

(23) Analytical data for the hydrosilylation products discussed matched those given in: (a) Fu, P.-F.; Brard, L.; Li, F. C.; Marks, T. J. *J. Am. Chem. Soc.* **1995**, *117*, 7157. (b) Rubin, M.; Schwier, T.; Gevorgyan, V. *J. Org. Chem.* **2002**, *67*, 1936.

(24) The fate of the resulting silylium cation is not known, but it might be stabilized by forming an adduct with the NMe_2 moiety.

of the present study nicely complement those of our previous studies on the importance of the amine moiety for catalytic activities; the lessons learned from these studies should lead to the development of highly active precatalysts bearing hemilabile amine moieties.

Experimental Section

General Comments. All manipulations were performed under an inert atmosphere of N_2 using standard Schlenk techniques and a drybox. Dry, oxygen-free solvents were employed throughout. Preparation of (η^3:η^0-Ind$(CH_2)_2NMe_2$)-Ni(PPh_3)Cl (**1**),[7a] [(η^3-η^1-Ind$(CH_2)_2NMe_2$)Ni(PPh_3)][BPh_4] (**7**),[7a] and $(PMe_3)_2NiCl_2$[8b] have been reported previously. LiCCPh has been prepared by deprotonation of HCCPh with BuLi in hexanes. All other reagents used in the experiments were obtained from commercial sources and used as received. The elemental analyses were performed by the Laboratoire d'Analyse Élémentaire (Université de Montréal). The spectrometers used for recording the NMR spectra are as follows: Bruker AMXR400 (^{1}H (400 MHz), $^{13}C\{^1H\}$ (100.56 MHz), and $^{31}P\{^1H\}$ (161.92 MHz)) and Bruker AV300 (^{1}H (300 MHz) and $^{31}P\{^1H\}$ (121.49 MHz)).

(η^3:η^0-Ind$(CH_2)_2NMe_2$)Ni(PMe_3)Cl (2). A THF solution of Ind$(CH_2)NMe_2$ (700 mg, 3.93 mmol) and BuLi (1.6 mL of a 2.5 M solution in hexane) was stirred for 3 h and then transferred (dropwise over 2 h) to a stirred solution of Ni$(PMe_3)_2Cl_2$ (1.1 g, 3.93 mmol) in 30 mL of THF at 50 °C. The resulting solution is evaporated and extracted with 90 mL of hot Et_2O. The Et_2O solution is reduced to 40 mL and cooled (−20 °C). Dark red powder (365 mg, 26% yield) precipitated as pure **2**. Recrystallization from hot hexane/Et_2O gave crystals suitable for X-ray diffraction analysis. $^{31}P\{^1H\}$ NMR (C_6D_6): −11.01 ppm. ^{1}H NMR (C_6D_6): 7.11 (d, $^3J_{H-H}$ = 7.7 Hz, H7), 6.99 (t, $^3J_{H-H}$ = 7.3 Hz, H5 or H6), 6.91 (t, $^3J_{H-H}$ = 7.3 Hz, H5 or H6), 6.59 (d, $^3J_{H-H}$ = 7.3 Hz, H4), 6.57 (H2), 3.66 (H3), 2.80 and 2.65 (m, IndCH_2), 2.38 and 2.29 (CH_2N), 2.17 (NCH_3), 0.74 (d, $^3J_{H-P}$ = 9.4 Hz, PCH_3). $^{13}C\{^1H\}$ NMR (C_6D_6): 130.0 (C7A), 126.5 (C3A), 125.8 (C4), 125.6 (C5), 118.4 (C6) 116.1 (C7), 104.4 (C1), 102.8 (C2), 59.8 (C3), 57.3 (*C*H_2N), 45.6 (N*C*H_3), 24.7 (Ind-*C*H_2), 14.7 (d, $^2J_{C-P}$ = 29.1 Hz, P*C*H_3). Anal. Calcd for $C_{16}H_{25}NPNiCl$: C, 53.91; H, 7.07; N, 3.93. Found: C, 53.73; H, 7.24; N, 3.77.

(η^3:η^0-Ind$(CH_2)_2NMe_2$)Ni(PCy_3)Cl (3). Complex **1** (500 mg, 0.92 mmol) and PCy_3 (390 mg, 1.38 mmol) were mixed together in 80 mL of Et_2O and stirred for 3 h. The solution was then concentrated to 40 mL and cooled to −20 °C. After 24 h, a dark red solid precipitated as pure **3** (480 mg, 93% yield). $^{31}P\{^1H\}$ NMR (C_6D_6): 37.02 ppm. ^{1}H NMR (C_6D_6): 7.06 (m, H7/H6), 6.90 (m, H5/H6), 6.76 (H2), 4.17 (H3), 2.87 and 2.67 (m, IndCH_2), 2.33 (CH_2N), 2.21 (NCH_3), 1.95−1.09 (m, PCy_3). $^{13}C\{^1H\}$ NMR (C_6D_6): 130.2 (C7A), 128.9 (C3A), 126.3 and 125.4 (C4/C5), 118.6 (C6/C7), 103.5 (C2), 102.7 (C1), 59.0 (*C*H_2N), 57.4 (C3), 45.7 (N*C*H_3), 35.2 (d, $^1J_{P-C}$ = 19.4 Hz, *i*-C), 30.1 (d, $^2J_{P-C}$ = 6.2 Hz, *o*-C), 27.9 and 27.8 (d, $^3J_{P-C}$ = 4.5 Hz, *m*-C), 26.7 (s, *p*-C), 24.8 (ind-*C*H_2). Anal. Calcd for $C_{31}H_{49}NPNiCl\cdot H_2O$: C, 64.32; H, 8.88; N, 2.42. Found: C, 64.24; H, 9.13; N, 2.07.

(η^3:η^0-Ind$(CH_2)_2NMe_2$)Ni(PPh_3)Me (4). A solution of MeLi (0.374 mL of a 1.5 M solution in hexane) was added dropwise to a solution of **1** (203 mg, 0.374 mmol in 60 mL of Et_2O) and stirred for 1 h. The mixture was then filtered and evaporated to dryness. Recrystallization from hot hexane gave pure product (80 mg, 41% yield) as dark red crystals suitable for X-ray diffraction analysis. $^{31}P\{^1H\}$ NMR (C_6D_6): 46.9 ppm. ^{1}H NMR (C_6D_6): 7.7−7.0 (PPh_3, H5/H6/H7), 6.54 (d, $^3J_{H-H}$ = 7.7 Hz, H4), 6.39 (H2), 4.22 (H3), 2.8−2.5 (m, CH_2N and IndCH_2), 2.19 (NCH_3), −0.65 (d, $^3J_{H-P}$ = 5.6 Hz, Ni−CH_3). $^{13}C\{^1H\}$ NMR ($CDCl_3$): 134.2 (*i*-C of PPh_3), 133.7 (d, $^2J_{P-C}$ = 19.0 Hz, *o*-C of PPh_3), 129.7 (*p*-C of PPh_3), 128.5, 127.9 (d, $^3J_{P-C}$ = 14.5 Hz, *m*-C of PPh_3), 122.0 (C5/C6), 119.9 and 119.6 (C3A/C7A), 116.7 and 115.7 (C4/C7), 100.4 (C2), 91.1 (C1), 75.3 (C3), 59.1 (*C*H_2N), 45.7 (N*C*H_3), 24.0 (Ind-*C*H_2), −18.3 (d, $^2J_{C-P}$ = 24.8 Hz, Ni−Me). Anal. Calcd for $C_{32}H_{34}NPNi$: C, 73.59; H, 6.56; N, 2.28. Found: C, 73.62; H, 6.83; N, 2.67.

Reaction of 4 with HBF_4. $HBF_4\cdot OEt_2$ (7 μL, 0.057 mmol) was added to a solution of **4** (27.8 mg, 0.053 mmol) in $CDCl_3$ (ca. 0.8 mL). The solution was then transferred to an NMR tube and shaken to ensure complete mixing, and the NMR spectra were recorded 10 min later. The $^{31}P\{^1H\}$ and ^{1}H NMR spectra showed characteristic signals of **7**. Addition of more $HBF_4\cdot OEt_2$ (14 μL, 0.114 mmol) provoked the decomposition of the product.

Reaction of 4 with HCl. HCl (17 μL of a 2 M solution in Et_2O, 0.8 equiv) was added to a solution of **4** (22.7 mg, 0.043 mmol) in $CDCl_3$ (ca. 0.8 mL). The solution was then transferred to an NMR tube and shaken to ensure complete mixing, and the NMR spectra were recorded 10 min later. The $^{31}P\{^1H\}$ and ^{1}H NMR spectra showed ca. 70% conversion of **4** into **1**.

(η^3:η^0-Ind$(CH_2)_2$NMe2)Ni(PPh_3)CCPh (5). A solution of LiCCPh (67 mg, 0.62 mmol in 15 mL of benzene) was added dropwise to a solution of **1** (270 mg, 0.50 mmol) in benzene (15 mL) and stirred for 2 h. The mixture was then concentrated to ca. 3 mL, hexanes (ca. 25 mL) were added, and the mixture was cooled to −20 °C to give a dark red solid. Repeated recrystallization gave pure product (152 mg, 50% yield). $^{31}P\{^1H\}$ NMR ($CDCl_3$): 38.8 ppm. ^{1}H NMR (C_6D_6): 7.7−7.0 (PPh_3, CCPh, H6 and H7), 6.82 (H5), 6.45 (H2), 6.14 (H4), 3.97 (H3), 3.13 and 2.91 (CH_2N), 2.91 (IndCH_2), 2.25 (NCH_3). $^{13}C\{^1H\}$ NMR ($CDCl_3$): 134.1 (d, $^2J_{P-C}$ = 10.4 Hz, *o*-C of PPh_3), 133.2 (d, $^1J_{P-C}$ = 45.8 Hz, *i*-C of PPh_3), 132.2, 131.1 (CCPh, *o*-C), 130.1 (*p*-C of PPh_3), 128.8, 128.5, 128.1 (d, $^3J_{P-C}$ = 9.7 Hz, *m*-C of PPh_3), 127.4 (CCPh, *m*-C), 125.0 and 124.5 (C5/C6/CCPh, *p*-C), 123.0, 121.3, 117.9, and 116.7 (C4/C7), 101.8 (C2), 100.1, 99.0, 74.6 (C3), 58.4 (*C*H_2N), 45.7 (N*C*H_3), 25.6 (Ind-*C*H_2). IR (KBr, cm^{-1}): 3050, 2924, 2099 (CC), 1591, 1477, 1431, 1383, 1095, 814, 745, 692, 530. Anal. Calcd for $C_{39}H_{36}NPNi\cdot H_2O$: C, 74.78; H, 6.12; N, 2.24. Found: C, 74.66; H, 6.23; N, 2.25.

(η^3:η^0-Ind$(CH_2)_2NMe_2$)Ni(PMe_3)Me (6). MeLi (0.7 mL of a 2 M solution in Et_2O, 1.32 mmol) was added slowly to a solution of **2** (314 mg, 0.88 mmol) in Et_2O (40 mL) and stirred for 45 min. Desoxygenated water (0.7 mL) was then added, and the mixture was stirred for 10 min, filtered, dried ($MgSO_4$), and evaporated to give crude **6** as a sticky solid. Compound **6** is quite unstable in solution, decomposing to form a black insoluble powder; this prevented us from obtaining analytically pure samples. However, a small batch of crystals suitable for X-ray analysis was obtained after multiple recrystallizations from hexane solutions. $^{31}P\{^1H\}$ NMR (C_6D_6): −3.99 ppm. ^{1}H NMR (C_6D_6): 7.23 (d, $^3J_{H-H}$ = 7.8 Hz, H7), 7.07 (m, H5 or H6), 7.01 (m, H5 or H6), 6.99 (H4), 6.24 (H2), 4.47 (H3), 2.75 (m, IndCH_2), 2.61 (CH_2N), 2.19 (NCH_3), 0.64 (d, $^3J_{H-P}$ = 9.0 Hz, PCH_3), −0.73 (d, $^3J_{H-P}$ = 6.3 Hz, Ni−CH_3). $^{13}C\{^1H\}$ NMR (C_6D_6): 126.7 (C7A), 122.0 (C4/C5), 120.9 (C3A), 116.4 and 116.2 (C6/C7), 100.0 (C2), 91.4 (C1), 70.1 (C3), 59.5 (*C*H_2N), 45.8 (N*C*H_3), 24.9 (Ind-*C*H_2), 16.1 (d, $^2J_{C-P}$ = 44.5 Hz, P*C*H_3), −21.7 (d, $^2J_{C-P}$ = 25.2 Hz, Ni−Me). Anal. Calcd for $C_{17}H_{28}NPNi$: C, 60.76; H, 8.40; N, 4.17. Found: C, 55.67; H, 8.44; N, 3.88.

Reaction of 6 with HBF_4. $HBF_4\cdot OEt_2$ (7 μL, 0.057 mmol) was added to a solution of **6** (27.8 mg, 0.053 mmol) in $CDCl_3$ (ca. 0.8 mL). The solution was then transferred to an NMR tube and shaken to ensure complete mixing, and the NMR spectra were recorded 10 min later. The $^{31}P\{^1H\}$ and ^{1}H NMR spectra showed characteristic signals of **8**. Addition of more $HBF_4\cdot OEt_2$ (14 μL, 0.114 mmol) provoked the decomposition of the product.

[(η^3:η^0-Ind$(CH_2)_2NMe_2$)Ni(PMe_3)][BPh_4] (8). A CH_2Cl_2 mixture of **2** (228 mg, 0.64 mmol) and $NaBPh_4$ (1.095 g, 3.2 mmol) was stirred at room temperature for 4 h and filtered. The orange filtrate was concentrated to ca. 1 mL, and hexanes (40 mL) were added to precipitate an orange-red solid, which

was filtered, redissolved in ca. 1 mL of CH_2Cl_2, and precipitated by adding Et_2O (40 mL). Filtration and washing with Et_2O gave pure **8** (282 mg, 69% yield). $^{31}P\{^1H\}$ NMR (CD_2Cl_2): −20.77 ppm. ^1H NMR (CD_2Cl_2): 7.42 (d, $^3J_{H-H}$ = 7.2 Hz, H5), 7.34 (*o*-H, BPh_4), 7.24 (m, H6 and H7), 7.04 (m, *m*-H, BPh_4), 6.89 (m, *p*-H, BPh_4), 6.79 (s, H2), 6.78 (d, $^3J_{H-H}$ = 8.5 Hz, H4), 4.29 (m, H3), 3.19 and 2.80 (m, IndCH_2), 2.32 and 2.05 (s, NCH_3), 2.19 and 1.94 (m, CH_2N), 1.12 (d, $^3J_{H-P}$ = 8.8 Hz, PCH_3). $^{13}C\{^1H\}$ NMR (CD_2Cl_2): 164,0 (4-line multiplet, J_{B-C} = 49.2 Hz, *i*-C, BPh_4), 136.0 (*m*-C, BPh_4), 129.2 and 127.5 (C5 and C6), 126.0 and 124.8 (C3A and C7A), 125.7 (*o*-C, BPh_4), 121.8 (*p*-C, BPh_4), 117.9 (C4 and C7), 107.5 C2), 107.1 (d, $^2J_{C-P}$ = 8.3 Hz, C1), 75.2 (d, $^3J_{C-P}$ = 4.1 Hz, *C*H_2N), 65.4 (C3), 52.8 and 50.3 (N*C*H_3), 24.5 (Ind-*C*H_2), 14.7 (d, $^2J_{C-P}$ = 28.4 Hz, P*C*H_3). Anal. Calcd for $C_{40}H_{45}NPNiB\cdot H_2O$: C, 72.98; H, 6.90; N, 2.13. Found: C, 72.93; H, 7.10; N, 2.14.

[(η^3:η^0-Ind(CH$_2$)$_2$NMe$_2$)Ni(PCy$_3$)][BPh$_4$] (9). The mixture of **3** (400 mg, 0.71 mmol) and $NaBPh_4$ (1.20 g, 3.57 mmol) in CH_2Cl_2 was stirred at room temperature for 4 h and then filtered. The red filtrate was concentrated to 1 mL and Et_2O (40 mL) added to precipitate a red solid, which was filtered and redissolved in ca. 1 mL of CH_2Cl_2 and precipitated by adding Et_2O (ca. 40 mL). Filtration and washing with Et_2O gave pure **9** (395 mg, 66% yield). Crystals suitable for X-ray analysis were obtained from a cold solution of **9** in CH_2Cl_2/Et_2O. $^{31}P\{^1H\}$ NMR (CD_2Cl_2): 24.88 ppm. ^1H NMR (CD_2Cl_2): 7.39 (d, $^3J_{H-H}$ = 7.3 Hz, H5), 7.30 (*o*-H, BPh_4), 7.21−7.10 (m, H6, H7, and H2), 7.01 (m, *m*-H, BPh_4), 6.87 (m, *p*-H, BPh_4), 6.79 (d, $^3J_{H-H}$ = 7.5 Hz, H4), 4.41 (m, H3), 3.10 and 2.80 (m, IndCH_2), 2.22 and 2.13 (s, NCH_3), 2.1−1.1 (m, CH_2N and P*Cy*$_3$). $^{13}C\{^1H\}$ NMR (CD_2Cl_2): 164.0 (4-line multiplet, J_{B-C} = 49.5 Hz, *i*-C, BPh_4), 135.9 (*m*-C, BPh_4), 131.8 and 130.6 (C3A and C7A), 128.8 and 128.3 (C5 and C6), 125.6 (*o*-C, BPh_4), 121.8 (*p*-C, BPh_4), 119.3 and 118.2 (C4 and C7), 107.8 C2), 106.0 (d, $^2J_{C-P}$ = 8.3 Hz, C1), 75.5 (s, *C*H_2N), 65.4 (C3), 52.0 (N*C*H_3), 34.9 (d, $^1J_{P-C}$ = 18.8 Hz, *i*-C), 30.4 and 29.8 (s, *o*-C), 27.6 (m, *m*-C), 26.2 (s, *p*-C), 23.0 (Ind-*C*H_2). Anal. Calcd for $C_{55}H_{69}NPNiB\cdot CH_2Cl_2$: C, 72.36; H, 7.70; N, 1.51. Found: C, 72.05; H, 7.81; N, 1.55.

Polymerization of Styrene. 8 (13.5 mg, 0.021 mmol) or **9** (15.5 mg, 0.018 mmol) and styrene (2000 equiv) were stirred at room temperature (Table 4, runs 3 and 5) or at 80 °C (runs 4 and 6) for 2 days in dichloroethane (6 mL). Removal of the solvent and unreacted styrene gave a white solid (run 3: 70 mg, 23 turnovers; run 4: 1.39 g, 630 turnovers; run 5: 128 mg, 57 turnovers; run 6: 670 mg, 350 turnovers), which was isolated and analyzed by GPC (THF). ^1H NMR ($CDCl_3$): 7.07 (br), 6.59 (br), 1.87 (br), 1.45 (br). $^{13}C\{^1H\}$ ($CDCl_3$): 145.4 (*ipso*-C), 128.0 (*o*- and *m*-C), 125.9 (*p*-C), 44.1 and 40.8 (alkyl chain).

Polymerization of Phenylacetylene. To a solution of the Ni precatalyst (ca. 0.0364 mmol) in 2 mL of THF was added phenylactylene (0.40 mL, 3.64 mmol, 100 equiv) and MAO (0.24 mL of a 10% ww solution in toluene, 10 equiv with respect to Ni), and the reaction mixture was stirred for 24 h at room temperature and under nitrogen. (No reaction is observed in the absence of MAO.) The reaction was quenched by adding a solution of ethanol/acetic acid; the resulting yellow precipitate (PPA, 5−10% yield) was filtered, washed with hexane, dried in vacuo, and analyzed by GPC (THF). ^1H NMR ($CDCl_3$): 6.94 (m, *m*- and *p*-H), 6.62 (d, $^3J_{H-H}$ = 6.8 Hz, *o*-H), 5.84 (s, vinylic H).

Dehydropolymerization of PhSiH$_3$. Addition of $PhSiH_3$ (2.0 mmol, 0.25 mL) to solid samples of **4**, **5**, or **6** (0.01 mmol) led to the evolution of gas (H_2), which was most vigorous with the mixture of **6**. Stirring the mixtures for 3 days gave thick oils consisting of various mixtures of cyclic and linear polysilanes, as determined by the ^1H NMR spectra: broad peaks at 5.6−5.1 ppm (cyclic) and 4.8−4.4 ppm (linear). The cyclic to linear ratio was determined for each case by integration of these peaks (25:75 for reaction with **4** and **6**; 78:22 for reaction with **5**), while the monomer conversion was determined relative to the PhSiH_3 signal at 4.22 ppm (ca. 90% for reactions of **4** and **5**; >95% for the reaction of **6**).

Hydrosilylation of Styrene. Preparation of PhCH(Me)(SiPhH$_2$). Styrene (140 μL, 1.2 mmol, 100 equiv) and $PhSiH_3$ (150 μL, 1.2 mmol, 100 equiv) were added to a solution of **7** (10.0 mg, 0.0121 mmol) in CD_2Cl_2 (ca. 0.8 mL). The sample was left to stand in an ultrasonic bath over 24 h, during which the original orange color changed to dark red. $^{31}P\{^1H\}$ NMR (CD_2Cl_2): 41.2 (br) and −4.9 (free PPh_3) ppm. The new signals in ^1H NMR (CD_2Cl_2): 4.59 (m, PhSiH_2), 2.82 (m, PhC*H*), 2.19 (d, $^3J_{H-H}$ = 7.56 Hz, PhCH(CH_3)). Monomer conversion: (determined by integration of the signals due to PhSiH_3 vs PhCH(Me)PhSiH_2) 70%.

The experiment was repeated in the same manner for the other precatalysts. For **8**: 100% conversion; $^{31}P\{^1H\}$ NMR (δ, CD_2Cl_2) −5.6 (br) and −19.7 (**8**). For **9**: 45% conversion; $^{31}P\{^1H\}$ NMR (δ, CD_2Cl_2) 58.9 (major) and 30.9 (trace). The reaction of **8** with 1000 equiv each of styrene and $PhSiH_3$ in CD_2Cl_2 led to similar results after 24 h (conversion 93%). No hydrosilylation was observed in $CDCl_3$.

Preparation of PhCH(Me)(SiPh$_2$H) and PhCH$_2$CH$_2$(SiPh$_2$H). Styrene (140 μL, 1.2 mmol, 100 equiv) and Ph_2SiH_2 (222 μL, 1.2 mmol, 100 equiv) were added to a solution of **8** (7.7 mg, 0.0121 mmol) in CD_2Cl_2 (ca. 0.75 mL). The sample was left to stand in an ultrasonic bath over 24 h, during which the original orange color changed to dark red. $^{31}P\{^1H\}$ NMR (δ, CD_2Cl_2): 28.3, 26.9, −5.5, −7.8, −19.6 (major). The new signals in ^1H NMR (δ, CD_2Cl_2): 5.27 (t, PhCH_2CH_2Si*H*Ph$_2$), 5.21 (d, PhCH(Me)(Si*H*Ph$_2$)), 3.14 (m, PhC*H*(Me)(SiHPh$_2$)), 3.05 (m, PhCH$_2$CH_2SiHPh$_2$), 1.82 (m, PhCH_2CH$_2$SiHPh$_2$), 1.77 (d, $^3J_{H-H}$ = 7.56 Hz, PhCH(*Me*)(SiHPh$_2$)). Total conversion 80%; ratio of PhCH(Me)(SiHPh$_2$)) to PhCH$_2$CH$_2$SiHPh$_2$ was 7:1.

Preparation of CH$_3$(CH$_2$)$_5$(SiPhH$_2$). The above protocol was carried out using 1-hexene (100 μL, 1.2 mmol, 100 equiv), $PhSiH_3$ (150 μL, 1.2 mmol, 100 equiv), and **8** (7.7 mg, 0.0121 mmol). $^{31}P\{^1H\}$ NMR (δ, CD_2Cl_2): 87.3, −4.9. The new signal in ^1H NMR (δ, CD_2Cl_2): 4.46 (t, Si*H*). Conversion: 20%.

Cyclic Voltammetry. Electrochemical measurements were performed on an Epsilon electrochemical analyzer using 0.002 M solutions of the Ni(II) complexes in a 0.1 M CH_3CN solution of *n*-Bu_4NPF_6. Cyclic voltammograms were obtained in a standard, one-compartment electrochemical cell using a graphite-disk electrode as working electrode, a platinum wire as the counter electrode, and an Ag−$AgNO_3$ (0.01 M in CH_3CN) reference electrode. The experiments were performed in the potential range of −2.8 to 0.8 V (CH_3CN) using a scan rate of 100 mV/s. Under these conditions, $E_{1/2}$ for the Fc^+−Fc couple was 90 mV.[25]

[(η^3:η^0-Ind(CH$_2$)$_2$NMe$_2$)Ni(PMe$_3$)(Py)][BPh$_4$] (10) in Equilibrium with 8. Pyridine (0.0371 mmol, 3.0 μL, 1.08 equiv) was added to a solution of **8** (22.0 mg, 0.0344 mmol) in CD_2Cl_2 (ca. 0.75 mL), allowed to stand for 15 min, and analyzed by ^1H and $^{31}P\{^1H\}$ NMR spectroscopy. By integrating the $^{31}P\{^1H\}$ NMR signals for **10** (−9.19 ppm) and **8** (−20 ppm) a 1:1 ratio was established. ^1H NMR (CD_2Cl_2): 7.6−6.9 (BPh_4, Ind, and Py), 6.43 (H2), 4.45 (br, H3), 2.55 and 2.28 (IndCH_2CH_2), 2.16 (s, NCH_3), 1.05 (d, $^3J_{H-P}$ = 8.8 Hz, PCH_3).

More pyridine (1.08 equiv, 3.0 μL, 0.0371 mmol) was then added to the above sample, and the NMR spectra were recorded 15 min later, showing a 2.3:1 ratio of **10** and **8**. Repeated addition of pyridine allowed the determination of the equilibrium constant: K_{eq} = 41 ± 6 M^{-1}. Evaporation of the solution to dryness gave back the starting complex **8**.

[(η^3:η^0-Ind(CH$_2$)$_2$NMe$_2$)Ni(PCy$_3$)(Py)][BPh$_4$] (11). Pyridine (0.0309 mmol, 2.5 μL, 1.02 equiv) was added to a solution of **9** (25.5 mg, 0.0302 mmol) in CD_2Cl_2 (ca. 0.75 mL), and the ^1H and $^{31}P\{^1H\}$ NMR spectra were recorded 15 min later. The

(25) Pavlishchuk, V. V.; Addison, A. W. *Inorg. Chem. Acta* **2000**, *298*, 97.

$^{31}P\{^1H\}$ NMR spectrum showed the disappearance of the signal for **9** (24.88 ppm) and the emergence of a new signal at 33.20 ppm. ^1H NMR (CD_2Cl_2): 8.27, 7.75, 7.65, 7.40, 7.20 (m, Py and Ind), 7.31 (*o*-H, BPh_4), 7.01 (m, *m*-H, BPh_4), 6.87 (m, *p*-H, BPh_4), 6.49 (d, H4), 4.68 (m, H3), 2.48 (m, IndCH_2), 2.13 (s, NCH_3), 1.8−0.9 (m, CH_2N and PCy_3). Removing the volatiles under vacuum and recording the $^{31}P\{^1H\}$ NMR spectrum of the redissolved solid showed that **11** remained as the main product.

Crystal Structure Determinations. Dark red crystals of **5** were obtained from a cold (−20 °C) THF/hexanes solution. The crystal data for **5** were collected on a Nonius CAD-4 diffractometer with graphite-monochromated Cu Kα radiation at 223(2) K using the CAD-4 software.[26] Refinement of the cell parameters was done with the CAD-4 software, while the data reduction used NRC-2 and NRC-2A.[27]

Dark red crystals of **2**, **4**, **6**, and **9** were obtained from cold solutions **2** in Et_2O/hexanes, **4** or **6** in hexanes, and **9** in CH_2Cl_2/Et_2O. The crystal data were collected on a Bruker AXS SMART 2K diffractometer with graphite-monochromated Cu Kα radiation at 223(2) K using SMART.[28] Cell refinement and data reduction used SAINT.[29] All five structures were solved by direct methods using SHELXS97[30] and difmap synthesis (SHELXL96).[31] The refinements were done on F^2 by full-matrix least squares. All non-hydrogen atoms were refined anisotropically, while the hydrogens (isotropic) were constrained to the parent atom using a riding model. Solving the structure of **5** entailed an interesting problem: the CC triple bond first obtained was much shorter than expected.[32] Careful inspection of the data revealed that the starting material **1** cocrystallized with **5** in a 9:91 ratio (also confirmed by NMR spectroscopy). Taking into account this ratio and solving for a THF molecule disordered over two positions (occupancy of 0.62 and 0.38) resulted in a good *R* factor (ca. 4.3%). The structure of **4** also contained a disordered solvent molecule of hexane, which was situated on the inversion point with two orientations (occupancy of 0.35 and 0.15). The relatively high *R* factor for the structure of **6** (ca. 7.5%) is due to poor quality of the crystals (small, twinned needles). Finally, the crystal structure of **9** presented a disorder on the chelated tether (two positions with occupancy of 0.72 and 0.28) and also contained a CH_2Cl_2 molecule disordered over three positions (occupancy of 0.20, 0.38, and 0.42). These disorders were solved and allowed an *R* factor of 4.41%. Crystal data and experimental details for **2**, **4**, **5**, **6**, and **9** are listed in Table 1, and selected bond distances and angles are listed in Table 2.

Acknowledgment. The Natural Sciences and Engineering Research Council of Canada, le Fond FCAR of Quebec, and the University of Montreal are gratefully acknowledged for financial support. H. Terrien is thanked for her help with the GPC.

Supporting Information Available: Complete details on the X-ray analysis of **2**, **4**, **5**, **6**, and **9**, including tables of crystal data, collection and refinement parameters, bond distances and angles, anisotropic thermal parameters, and hydrogen atom. This material is available free of charge via the Internet at http://pubs.acs.org.

OM0341348

(26) *CAD-4 Software*, Version 5.0; Enraf-Nonius: Delft, The Netherlands, 1989.

(27) Gabe, E. J.; Le Page, Y.; Charlant, J.-P.; Lee, F. L.; White, P. S. *J. Appl. Crystallogr.* **1989**, *22*, 384.

(28) *SMART*, Release 5.059; Bruker Molecular Analysis Research Tool, Bruker AXS Inc.: Madison, WI 53719-1173, 1999.

(29) *SAINT*, Release 6.06; Integration Software for Single Crystal Data, Bruker AXS Inc.: Madison, WI 53719-1173, 1999.

(30) Sheldrick, G. M. *SHELXS*, Program for the Solution of Crystal Structures; University of Goettingen: Germany, 1997.

(31) Sheldrick, G. M. *SHELXL*, Program for the Refinement of Crystal Structures; University of Goettingen: Germany, 1996.

(32) Twenty-four structures containing a Ni−C≡C group have been found on the Cambridge Structural Database with a mean C≡C distance of 1.204 Å.